Enhanced D-Alpha H-mode Studies in the Alcator C-Mod Tokamak

E. Marmar, R.L. Boivin, C. Fiore, J. Goetz, R. Granetz, M. Greenwald, A. Hubbard, J. Hughes, I. Hutchinson, J. Irby, B. LaBombard, Y. Lin, B. Lipschultz, A. Mazurenko, D. Mossessian, T. Sunn Pedersen, M. Porkolab, J. Rice, G. Schilling[*], J.A. Snipes, G. Taylor[*], J. Terry, S. Wolfe, S. Wukitch

MIT Plasma Science and Fusion Center, Cambridge, MA, USA 02139
[*]Princeton Plasma Physics Laboratory, Princeton, NJ, USA 08543

e-mail contact for main author: Marmar@psfc.mit.edu

Abstract. A favorable regime of H-mode confinement, seen on the Alcator C-Mod tokamak is described. Following a brief period of ELM-free H-mode, the plasma evolves into the Enhanced D-Alpha (EDA) H-mode which is characterized by very good energy confinement, the complete absence of large, intermittent type I ELMs, finite impurity and majority species confinement, and low radiated power fraction. Accompanying the EDA H-mode, a quasi-coherent (QC) edge mode is observed, and found to be responsible for particle transport through the edge confinement barrier. The QC-mode is localized within the strong density gradient region, and has poloidal wavenumber $k_\theta \approx 5$ cm^{-1} and lab-frame frequency of ≈100 kHz. Parametric studies show that the conditions which promote EDA include moderate safety factor ($q_{95}>3.5$), high triangularity ($\delta>0.35$) and high target density ($n_e>1.2\text{x}20$ m^{-3}). EDA H-mode is readily obtained in purely ohmic and well as in ICRF auxiliary-heated discharges.

1. Introduction

Discharges with an H-mode edge transport barrier on the Alcator C-Mod tokamak[1] are usually seen to evolve from an ELM-free phase to a regime with quasi-coherent fluctuations in the barrier region, which we have called Enhanced D-Alpha (EDA) H-mode.[2] EDA H-mode is characterized by good energy confinement time (~$0.8\text{x}\tau_{\text{ELM-free}}$), combined with substantially reduced particle and impurity confinement times relative to those seen in ELM-free cases. There are no large discrete type I ELMs observed in Alcator C-Mod. This combination of features promises a path to steady-state edge barrier operation, without the impediment of impurity accumulation characteristic of ELM-free H-mode, while also avoiding intermittent bursts of power outflux which challenge divertor design for next-generation devices.[3] Detailed fluctuation measurements in the pedestal region show the onset of a quasi-coherent (QC) mode which is always present during all EDA phases of discharges, and which is absent at all other times. Direct probe measurements of density and electric field fluctuations reveal that the mode is responsible for much, if not all, of the observed enhancement in particle transport which accompanies EDA H-mode. Magnetic pickup measurements made just outside of the separatrix show that the quasi-coherent mode has a strong magnetic component. Phase Contrast Imaging measurements, which are confirmed by the probes, show that the QC mode has a short poloidal wavelength (~1 cm). The short wavelenth of the QC mode distinguishes it from ELM precursors. EDA H-mode may bear some similarities to the small or no-ELM regimes which have been observed on other tokamaks, including LPC H-Mode on JET,[4] and type II or grassy ELM H-Modes seen on DIII-D [5] and JT-60U,[6] but the exact relationships among these different regimes is presently unclear.

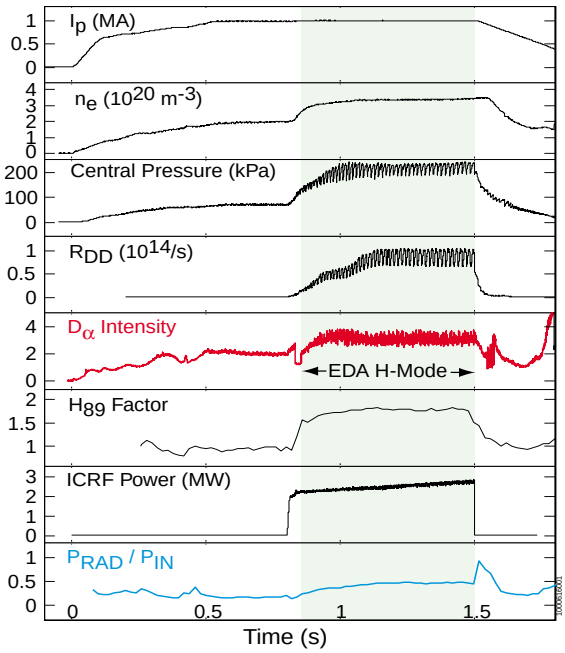

FIG. 1. Time histories of plasma parameters for a typical EDA H-Mode discharge. The plasma is in the EDA mode during the shaded time. Note that all plasma parameters come into steady-state.

2. Plasma Properties of EDA H-mode

Time traces for typical plasma parameters of a C-Mod discharge are shown in figure 1. In this case, 80 MHz ICRF H minority heating, in a D majority plasma, is applied beginning at 0.8 seconds. The on-axis magnetic field is 5.3 T, putting the ICRF resonance at the center of the plasma. The plasma makes a transition into H-mode 20 ms after 2 MW of auxiliary heating is applied, as seen by the sharp drop in the D_α intensity. At the same time, the electron density begins to rise. The initial phase is a standard ELM-free H-mode; 23 ms after the transition, there is a rise in the D_α, as the plasma enters the EDA phase. In sharp contrast to ELM-free cases, the density reaches a new plateau value, and at the same time impurity levels and radiated power also stop increasing. The global energy confinement during the steady state portion reaches 0.06 s, corresponding to $\tau_E/\tau_{ITER\text{-}89P}$ = 1.85. As shown in figure 2, which compares τ_E for a series of ELM-free and EDA cases, the energy confinement is only slightly reduced for the EDA cases. Experiments with injected trace non-recycling impurities show that impurity particle confinement is essentially infinite, on the time scale of the ELM-free discharges, while for EDA, this time is typically reduced to about 0.2 second, corresponding to about $5 \bullet \tau_E$. EDA H-mode is obtained in both ohmic and ICRF heated H-mode discharges.[7] This implies that the phenomenon is not related to fast particle or other ICRF effects.

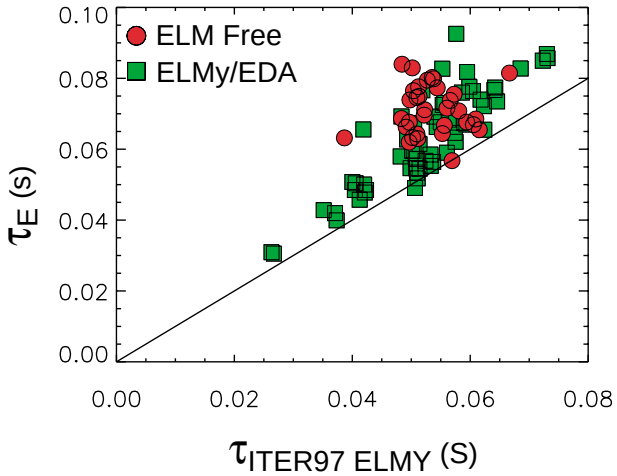

FIG. 2. Comparison of energy confinement scaling for ELM-free and EDA H-Mode discharges. The results are compared with one of the scalings from the ITER database.

3. Quasi-coherent Edge Mode

Detailed edge fluctuation measurements have revealed the probable cause for the main differences between ELM-free and

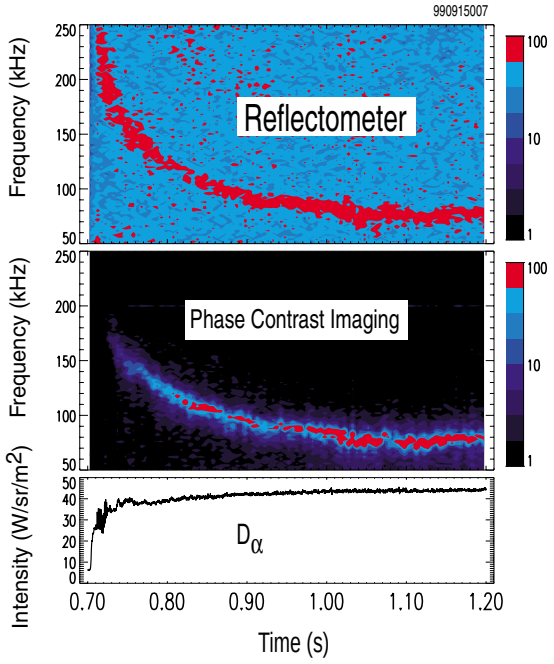

FIG. 3. Time histories of density fluctuation spectra as seen on the reflectometer and phase contrast imaging diagnostics.

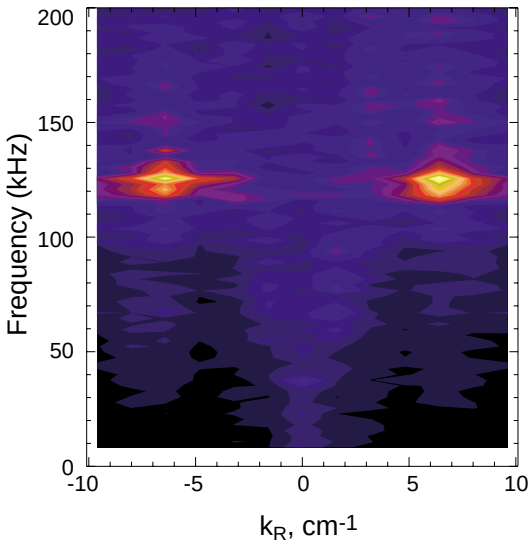

FIG. 4. Wavenumber for the QC mode as measured with the PCI diagnostic. The two lobes, at positive and negative k, correspond to the 2 edges viewed by the PCI chords.

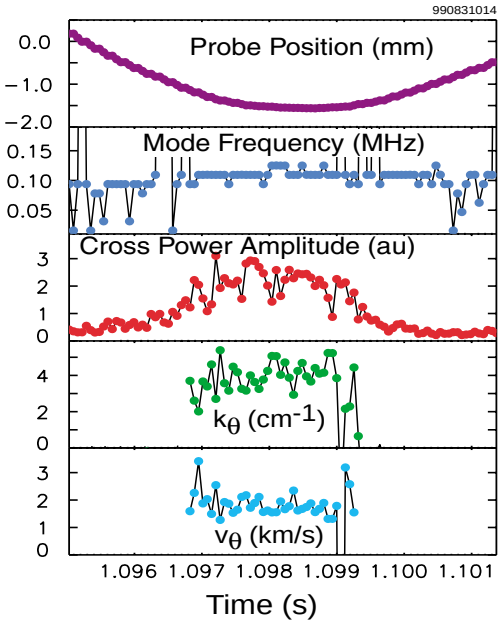

FIG. 5. Time histories of QC mode parameters measured with fast-scanning langmuir probes. The probe head scans in from outside the separatrix, and the mode appears when the probe is in the pedestal region.

EDA behavior. A strong, quasi-coherent (QC) mode is universally correlated with EDA periods in C-Mod plasmas. With a lab-frame frequency in the 100 kHz range, the QC mode is seen in density, potential and magnetic fluctuation measurements. Figure 3 shows the spectral time history of the density fluctuations, as seen with reflectometry[8] and phase contrast imaging (PCI).[9] After a brief ELM-free period, the mode appears, at around 250 kHz, coincident with the increase in D_α and increases in particle transport. The frequency decreases, most likely due to changes in the poloidal rotation inside the H-mode barrier region, reaching a steady-state value after about 0.2 second. The PCI diagnostic images the plasma through 12 adjacent vertical chords, yielding measurements of the mode wavenumber, k, in the major radius direction. Since the mode is localized at the plasma boundary, this is interpreted as corresponding to k_θ. Figure 4 illustrates the results of a PCI measurement of k, showing the (f, k) dispersion over a narrow time window in a single discharge. The poloidal wavenumber has a value of about 6 cm^{-1}, corresponding to a wavelength of about

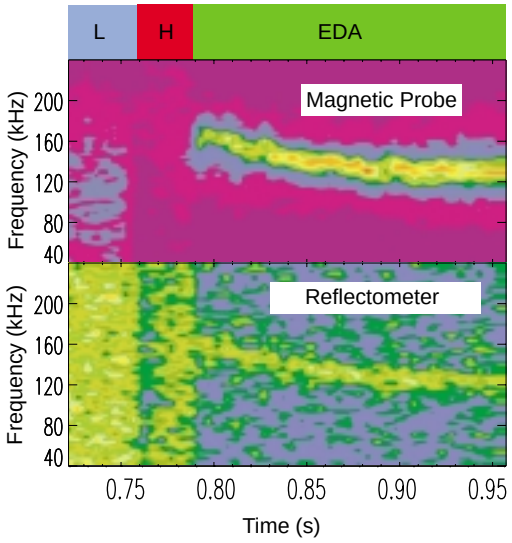

FIG. 6. Comparison of magnetic and density fluctuation spectra for the QC mode.

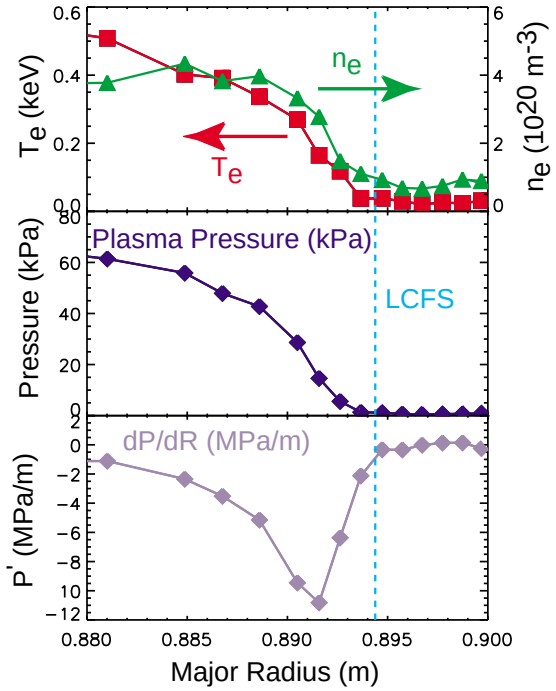

FIG. 7. T_e and n_e profiles from high resolution edge Thomson scattering. The pressure profile is constructed assuming T_i=T_e.

1 cm. There are 2 lobes present in the dispersion, because the diagnostic integrates through the pedestal at both the top and bottom edges of the plasma.

Electrostatic measurements taken with a set of fast-scanning Langmuir probes have confirmed the k measurements. The mode is only seen on the probes when they are inserted directly into the H-mode pedestal region, as illustrated in figure 5. Utilizing adjacent probes on the same scanning head, it is possible to measure directly the poloidal component of **k**, and one such result is shown in the fourth panel of the figure. The bottom panel shows the phase velocity obtained from the same data, which is found to be in the electron diamagnetic direction. Measurements of $< \tilde{n} \cdot \tilde{E} >$ show that the mode drives cross-field particle flux, in reasonable quantitative agreement with the observed fluxes inferred from density profiles.

Possible magnetic components in the QC mode were investigated by adding a magnetic pickup loop to one of the fast scanning probes. A typical spectral time history from the magnetic measurement is shown in figure 6. In this case, the probe was positioned so that the center of the pickup coil was about 20 mm outside of the separatrix. A very clear magnetic fluctuation is evident, with exactly the same frequency time history as that seen in the density fluctuations. The value of dB/dt at the probe location for this shot was 50 tesla/second. Radial scans show a very fast fall-off in dB/dt, going approximately as $(1/r)^{35}$. Extrapolating these results into the center of the transport barrier yields an estimate for the perturbed current density at the mode location of about 10 A/cm^2.

4. Pedestal Profiles and MHD Limits

Detailed measurements of density, temperature and impurity profiles have been made for the H-Mode pedestals in both ELM-free and EDA cases. Pedestal widths are typically in the few mm range, and the measured electron pressure gradients are very high, approaching 10^7 Pascal/m in the highest ICRF power cases. Electron density and temperature profiles from

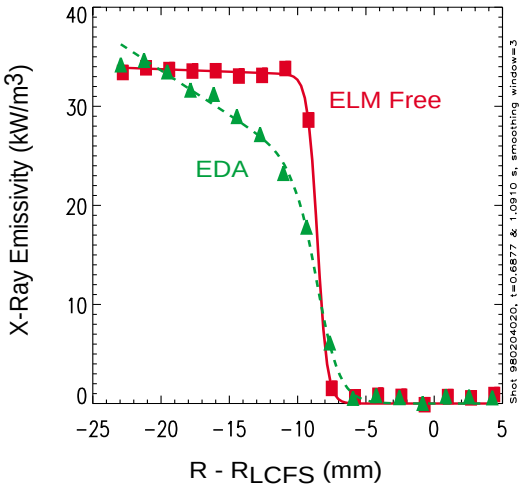

FIG. 8. Soft x-ray profiles comparing ELM-free and EDA discharges.

a high resolution edge Thomson scattering system[10] are shown for an EDA discharge in figure 7. T_i profiles are not yet measured in the pedestal, but assuming $T_i = T_e$, total plasma pressure profiles are inferred, and also plotted in the figure. Modeling with the BALOO MHD stability code[11] indicates that these profiles are generally at, or in some cases, well above the ideal first stability β limit for ballooning modes. Nevertheless, type I ELMs are not seen. While still under investigation in the modeling, it is likely that edge bootstrap current driven in the strong pedestal region opens up a path to second stability, reminiscent of the picture developed from DIII-D.[12] The profiles of T_e and n_e show little or no systematic differences when comparing ELM-free to EDA regimes. One profile which is clearly different is related to impurity density. High resolution soft x-ray imaging[13] reveals that the impurity pedestal is significantly narrower in ELM-free than in EDA. An example comparing two x-ray emissivity profiles is shown in figure 8. In these cases, the measured emissivity has been shown to be directly related to the product of $n_e \cdot n_I$, where n_I, the impurity density, is dominated by highly stripped fluorine, one of the trace impurities in the plasma. Because the x-ray pedestal is located about 5 mm inside the n_e pedestal, n_e is nearly constant across the region of interest, and the emissivity gradient is due almost entirely to the impurity density profile. It is clear from the figure that a major difference between the EDA and ELM-free regimes is the broadening of the edge impurity profile, which in turn is directly related to the degraded impurity confinement, which is one of the very desirable properties of the EDA H-mode.

5. Conditions Favoring EDA Formation

Under many circumstances, the H-mode discharges on Alcator C-Mod evolve from ELM-free to EDA. Systematic parameter scans have been performed in an attempt to understand the underlying physical mechanism(s) responsible for triggering and sustaining the QC mode which appears to be responsible for the EDA phenomena. Several trends have emerged from these studies. EDA formation is favored for discharges with: moderate safety factor ($q_{95}>3.5$); stronger triangularity ($\delta>0.35$); higher target plasma density ($\bar{n}_e > 1.2\times10^{20} m^{-3}$). Scans of elongation indicate that, at least over a relatively small range ($1.55<\kappa<1.75$), κ is not a strongly controlling parameter. Finally, impurity radiation can also prevent the transition into EDA, or cause a reversion from EDA back to ELM-free, typically when $P_{rad}/P_{in}>0.7$. Collisionality may be one of the key plasma parameters determining the EDA/ELM-free boundary, but more definitive conclusions in this regard await further investigations.

6. Summary

Many aspects of the favorable Enhanced D-Alpha H-mode, seen on the Alcator C-Mod tokamak have been studied. EDA H-mode combines very good energy confinement, with the absence of impurity accumulation. In contrast to type I ELMy behavior, edge pressure and density are controlled in a continuous fashion. A quasi-coherent mode has been identified which appears to be responsible for the enhanced majority and impurity particle transport. The mode has relatively short wavelength (1 cm), and typical lab-frame frequency of 100 kHz. The mode has a strong magnetic component. Direct density and electric field fluctuation measurements, made in the high gradient pedestal region with electrostatic probes, show that the mode is responsible for outgoing particle flux. Plasma shaping, density and magnetic shear all appear to play a role in defining the EDA/ELM-free operational boundaries. EDA H-mode is readily obtained in ohmic-only as well as in ICRF auxiliary-heated discharges, ruling out the possibility that EDA is caused by fast particle or other RF driven phenomena.

Acknowledgements

This work supported by the US Department of Energy.

References

[1] HUTCHINSON, I.H., et al., Phys. Plasmas **1** (1994) 1511.
[2] GREENWALD, M.J., et al., Phys. Plasmas **6** (1999) 1943.
[3] LEONARD, A.W., et al., J. Nuclear Materials **266-269** (1999) 109.
[4] BURENS, M., et al., Nucl. Fusion **32** (1992) 539.
[5] OZEKI, T., et al., Nucl. Fusion **30** (1990) 1425.
[6] KAMADA, Y., et al., Plasma Phys. Control. Fusion **38** (1996) 1387.
[7] GREENWALD, M., et al., Plasma Phys. Control. Fusion **42** (2000) A263.
[8] LIN, Y., et al., Rev. Sci. Instrum. **70** (1999)1079.
[9] MAZURENKO, A., et al., Bull. Am. Physical Soc. **44** (1999) 257, paper RO2 10.
[10] HUGHES, J.W., et al., Proceedings of the 13th Topical Conference on High Temperature Plasma Diagnostics, Tucson, Arizona, 18-22 June, 2000, Rev. Sci. Instrum. to be published.
[11] MILLER, R.L., et al., Phys. Plasmas **4** (1997) 1062.
[12] FERRON, J., et al, Phys. Plasmas **7** (2000) 1976.
[13] PEDERSEN, T. Sunn, et al., Nucl. Fusion **40** (2000) 1795.